Journal of Organometallic Chemistry, 401 (1991) 227–243
Elsevier Sequoia S.A., Lausanne
JOM 21272

Metalloporphyrins with metal–metal σ-bonds. Synthesis, spectroscopic characterization, and electrochemistry of $(P)MRe(CO)_5$ where P is the dianion of octaethylporphyrin (OEP) or tetraphenylporphyrin (TPP) and M = Al, Ga, In or Tl

Roger Guilard * [a], Abdellah Zrineh [a,b], Alain Tabard [a], Laurent Courthaudon [c], Baocheng Han [c], Mohammed Ferhat [b] and Karl M. Kadish *[c]

[a] *Laboratoire de Synthèse et d'Electrosynthèse Organométalliques Associé au CNRS (URA 33), Faculté des Sciences "Gabriel", 6, Boulevard Gabriel, Université de Bourgogne, 21100 Dijon (France)*
[b] *Laboratoire de Chimie Physique Générale, Faculté des Sciences de Rabat, Université Mohammed V, Rabat (Morocco)*
[c] *Department of Chemistry, University of Houston, Houston, TX 77204-5641 (USA)*

(Received June 25th, 1990)

Abstract

The synthesis, physicochemical properties, and electrochemistry of a new series of metal–metal σ-bonded metalloporphyrins are reported. The investigated compounds are represented as $(P)MRe(CO)_5$ where P is the dianion of octaethylporphyrin (OEP) or tetraphenylporphyrin (TPP) and M = Al, Ga, In, or Tl. These compounds provide the first examples of Al and Ga metalloporphyrins with covalent metal–metal bonds as well as give the first series of compounds in which the same metalate anion is covalently bonded to four different group 13 metalloporphyrins. Each synthesized complex was characterized by ^1H NMR, IR, and UV-visible spectroscopy as well as by electrochemistry. Graham $\Delta\sigma$ and $\Delta\pi$ parameters, and calculated residual charges on the rhenium atom of $(P)MRe(CO)_5$ demonstrate that the covalency of the metal–metal bond decreases in the order: $Tl \gg In > Ga > Al$. The thallium derivative is stable upon electrooxidation by either one or two electrons. However, the In, Ga, and Al complexes undergo rapid cleavage of the metal–rhenium bond after formation of a $[(P)MRe(CO)_5]^{+\cdot}$ cation radical. The chemical reactivity and physical properties, as well as the electrochemistry, of each $(P)MRe(CO)_5$ species were analyzed as a function of the central metal ion or porphyrin ring basicity. The spectroscopic properties and electrochemistry of these metal–metal σ-bonded species are compared with data for other metal–metal bonded metalloporphyrins of the type (P)MM′(L) as well as with data for related metal–carbon bonded porphyrins of the type (P)M(R).

Introduction

Numerous metal–metal bonded metalloporphyrins have been synthesized to better understand biological processes, or as starting derivatives in the preparation of new materials [1–19]. One family of these organometallic species which has been

0022-328X/91/$03.50

characterized in the literature includes σ-bonded bimetallic metalloporphyrins of the type (P)MM′(L) where P is the dianion of a given porphyrin ring, M is In or Tl, and M′(L) is a metalate anion such as $Mn(CO)_5$, $Co(CO)_4$, $Cr(CO)_3Cp$, $Mo(CO)_3Cp$, or $W(CO)_3Cp$ [1–3,6–9].

The stability of a given (P)MM′(L) or (P)M(R) derivative will depend upon the covalent character of the metal–metal or metal–carbon bond; the more covalent the bond, the more stable will be the complex. The most stable group 13 σ-bonded porphyrins which have been synthesized to date are those with a Tl central metal ion [8] while the least stable are carbon σ-bonded complexes of the type (P)Al(R) [10] or (P)Ga(R) [11], where R is an alkyl or aryl group. All attempts to synthesize aluminum or gallium metalloporphyrins with σ-bonded $Mn(CO)_5$, $Co(CO)_4$, or $M(CO)_3Cp$ axial ligands have so far proven to be unsuccessful.

Previous work on bimetallic indium [1–3,6,7] and thallium [1–3,8] porphyrins has demonstrated that the metal–metal bond strength of a given complex parallels the nucleophilic character of the metalate anion. Dessy et al. [12] reported that the anion nucleophilicity of $Re(CO)_5^-$ is greater than that of either $Mn(CO)_5^-$ or $Co(CO)_4^-$, both of which can form bimetallic complexes with In or Tl metalloporphyrins [1–3,6–9]. This fact therefore led us to attempt the synthesis of $(P)MRe(CO)_5$ complexes.

In this present paper we report the synthesis, physicochemical properties, and electrochemical characterization of seven group 13 metalloporphyrins containing a σ-bonded $Re(CO)_5$ ligand. The investigated compounds are represented as $(P)MRe(CO)_5$ where P = OEP or TPP and M = Al, Ga, In or Tl. The present series of compounds provides the first examples of gallium and aluminum porphyrins with covalent metal–metal bonds as well as gives the first example where the same metalate anion can be σ-bonded to four different group 13 metalloporphyrins. Each derivative was characterized by IR, UV-visible, and ^1H NMR spectroscopy as well as by electrochemistry. The spectroscopic properties and electrochemistry of these metal–metal σ-bonded species are compared with data for other metal–metal bonded metalloporphyrins of the type (P)MM′(L), as well as with data for related metal–carbon σ-bonded porphyrins of the type (P)M(R).

Experimental

Chemicals. Synthesis and handling of each bimetallic porphyrin complex and metalate anion were carried out under an argon atmosphere. All common solvents were thoroughly dried in an appropriate manner [13] and distilled under argon prior to use. The starting (P)MCl species, were prepared by metalation of $(OEP)H_2$ or $(TPP)H_2$ according to literature methods [14]. $NaRe(CO)_5$ was synthesized by sodium amalgam reduction of $Re_2(CO)_{10}$ in tetrahydrofuran under an inert argon atmosphere [15]. Spectroscopic grade methylene chloride (CH_2Cl_2, Fisher) was used for electrochemical studies and was distilled from P_2O_5 prior to use. Tetrabutylammonium hexafluorophosphate ($TBA(PF_6)$) was purchased from Alfa. This supporting electrolyte was twice recrystallized from absolute ethyl acetate and dried in a vacuum oven at 40 °C prior to use.

General procedure for preparation of (P)MRe(CO)$_5$ where M = Al, Ga, In, or Tl. $NaRe(CO)_5$ in THF (23 cm^3, 0.7 mmol) was added dropwise to (P)InCl or (P)TlCl (0.5 mmol) in tetrahydrofuran (150 cm^3) at room temperature in the dark and gave

Table 1

Yield (%) and analytical data for (P)MRe(CO)$_5$ complexes

Porphyrin, P	Central metal	Molecular formula	Recrystallization solvent [a]	Yield, (%)	Anal. data (%) [b]		
					C	H	N
OEP	Al	$C_{41}H_{44}N_4AlReO_5$	[c]	47 [d]	–	–	–
	Ga	$C_{41}H_{44}N_4GaReO_5$	A/B (2/1)	49	53.5 (53.02)	4.0 (4.78)	4.8 (6.03)
	In	$C_{41}H_{44}N_4InReO_5$	A/B (2/1)	79	52.0 (50.56)	4.7 (4.56)	5.5 (5.75)
	Tl	$C_{41}H_{44}N_4TlReO_5$	A/B (2/1)	90	44.6 (46.31)	4.2 (4.18)	5.1 (5.27)
TPP	Ga	$C_{49}H_{28}N_4GaReO_5$	A/B (2/1)	59	57.6 (58.34)	2.8 (2.80)	5.5 (5.55)
	In	$C_{49}H_{28}N_4InReO_5$	A/B (2/1)	88	53.6 (55.84)	2.6 (2.68)	5.2 (5.31)
	Tl	$C_{49}H_{28}N_4TlReO_5$	A/B (2/1)	94	50.5 (51.47)	2.4 (2.47)	4.9 (4.90)

[a] Abbreviations: A = benzene, B = heptane. [b] Calculated values in parentheses. [c] Compound could not be recrystallized (see text). [d] Crude compound.

(P)InRe(CO)$_5$ or (P)TlRe(CO)$_5$ as a final product. The same procedure was used for preparation of (P)AlRe(CO)$_5$ and (P)GaRe(CO)$_5$, but these syntheses were carried out in toluene at $-70\,^{\circ}$C.

The formation of each bimetallic complex was monitored by UV-visible spectroscopy and the reaction stopped after about one hour. The solutions were then chromatographed in the dark over a short, silica gel-packed column under an argon atmosphere (eluent: toluene; column dimensions: 3 cm × 3 cm; silica gel 20–210 mesh). After solvent evaporation, the crude product was recrystallized from a benzene/heptane mixture. Yields are given in Table 1 and varied from 47 to 94% depending upon the specific central metal ion and the porphyrin macrocycle.

Instrumentation. Elemental analyses were performed by the Service de Microanalyses du C.N.R.S.. ^{1}H NMR spectra were recorded at 400 MHz on a Bruker WM 400 spectrometer of the Cerema (Centra de Résonance Magnétique de l'Université de Bourgogne). Spectra were measured from 5 mg solutions of the complex in C_6D_6 with tetramethylsilane as internal reference. Infrared spectra were obtained on a Perkin Elmer 580 B apparatus. Solid samples were prepared as a 1% dispersion in CsI pellets. Electronic absorption spectra were recorded on a Perkin Elmer 559 spectrophotometer or an IBM Model 9430 spectrophotometer.

Electrochemistry was carried out with the use of a three-electrode system. The working electrode was a platinum button which had a diameter of 0.1 cm. The counter electrode was a platinum wire. A home-made saturated calomel electrode (SCE) was used as reference and was separated from the bulk of the solution by a fritted glass bridge. Cyclic voltammograms were obtained with an IBM Model EC 225 voltammetric analyzer coupled with a Houston Instrument Model 2000 X–Y recorder. High-purity nitrogen was used for deaeration and to maintain an N_2 atmosphere above the solution during the experiment. Electrochemical data were collected in the dark in order to minimize photocleavage of the metal–metal bond.

Results and discussion

Seven different (P)MRe(CO)$_5$ complexes were synthesized in the reaction between (P)MCl and Re(CO)$_5^-$. The analytical data of the resulting (P)MRe(CO)$_5$ species are summarized in Table 1 and are consistent with the calculated molecular formulas. Significant differences in the yield of a given complex were obtained depending upon the specific central metal ion and the type of porphyrin macrocycle. (P)InRe(CO)$_5$ and (P)TlRe(CO)$_5$ were isolated at room temperature in yields between 79 and 94% while the aluminum and gallium derivatives could only be obtained at low temperature ($-70\,^\circ$C) and were isolated in lower yields which ranged between 47 and 59%. The TPP derivatives of Ga, In, and Tl are obtained in higher yields than the OEP complexes with the same central metal. For the case of the Al derivatives, the OEP complex appeared to be more stable than the TPP species. However, some problems were encountered with either purification or isolation of both complexes. (OEP)AlRe(CO)$_5$ could not be recrystallized and only the crude product was obtained for spectroscopic and electrochemical characterization. Although all attempts to isolate (TPP)AlRe(CO)$_5$ were unsuccessful, its formation could be monitored by UV-visible spectroscopy. The overall stability of a given (P)MRe(CO)$_5$ complex with the same porphyrin ring and a different central metal thus follows the sequence: Al < Ga < In $\ll$ Tl. The same order of stability is also observed for (P)MM'(L) where M = In or Tl and M'(L) = Co(CO)$_4$, Mn(CO)$_5$, or M''(CO)$_3$Cp where M'' = Cr, Mo or W [1–3].

Spectral characterization of neutral (P)MRe(CO)$_5$. Infrared spectral data for (P)MRe(CO)$_5$ in both the solid state and in solution are listed in Tables 2 and 3. IR spectra of (TPP)GaRe(CO)$_5$ under both conditions are illustrated in Figure 1 which covers only the carbonyl stretching vibration region.

The solid state IR spectrum of (P)MRe(CO)$_5$ is typical of a metal carbonyl complex [16–19]. The CO stretches range from 1942 to 2114 cm^{-1} while the ReCO bands and ReC stretches appear close to 590 and 400 cm^{-1}, respectively (see Table 2). The symmetry of the axial Re(CO)$_5$ group can be determined from the number of bands in the CO stretching region [18]. Four to six CO vibrations are observed, depending upon the nature of the porphyrin macrocycle (see Figure 1a and Table 2). These absorptions are consistent with C_s local symmetry around the rhenium atom. The stronger electron donation of the OEP ring in (OEP)MRe(CO)$_5$ induces a small shift of the ν_{CO} bands towards lower wavenumbers when compared to (TPP)MRe(CO)$_5$ and indicates that the electron density on the five CO groups of the various complexes is slightly increased for the octaethylporphyrin derivatives.

The IR data for (P)MRe(CO)$_5$ may be compared to spectral data for (P)InMn(CO)$_5$ [6,7,9] and (P)TlMn(CO)$_5$ [8], since all three types of complexes have similar symmetry. The δ_{ReCO} and ν_{ReC} bands of (P)MRe(CO)$_5$ appear at lower wavenumbers than the corresponding vibrations of the (P)MMn(CO)$_5$ complexes ($\Delta(\delta_{MCO}) \approx 60$ cm^{-1}, $\Delta(\nu_{MC}) \approx 75$ cm^{-1}) [20*]. This variation can be attributed to differences in the nature of the specific metalate anion which induces changes in the σ and π bonding properties. However, the position of the carbonyl absorptions

* Reference number with asterisk indicates a note in the list of references.

can also depend upon local symmetry as was reported for several non-porphyrin rhenium compounds [16,21–24].

The CO stretching constants (k_1, k_2) and the CO–CO interaction constants (k) [25*] were calculated for each (P)MRe(CO)$_5$ complex by the Cotton–Kraihanzel method [26] and are listed in Table 3. There are two bands for each compound between 1981 and 2113 cm^{-1}, with the strongest one appearing at lower wavenumbers (see Figure 1b). This is consistent with the metalate ligand possessing a higher symmetry in solution than in the solid state, i.e. a C_{4V} local symmetry in solution [17–19]. Three infrared-active carbonyl stretching modes ($2A_1 + E$) and one Raman-active mode (B_1) are expected for such a symmetry. The calculated force constants indicate that the medium intensity band at the highest wavenumbers (ν_1) can be assigned to the A_1 mode while the strongest absorption at the lowest wavenumbers belongs to the E mode. The second A_1 mode is probably overlapped by the strong absorption E [26,27]. Some of the complexes also show a weak intensity absorption between ν_1 and ν_2. This is illustrated in Figure 1b for (TPP)GaRe(CO)$_5$. This band is attributed to the B_1 mode and implies a lower symmetry than C_{4V} [22]. The good agreement between the calculated and experimental position of this absorption confirms the assignment.

In order to define the influence of the porphyrin unit, Graham's parameters were calculated by using equations 1 and 2 [28]. (CH$_3$)Re(CO)$_5$ was chosen as the reference derivative ($k_1 = 16.05$ mdyn/Å and $k_2 = 16.90$ mdyn/Å) [17,29].

$$\Delta k_1 = \Delta\sigma + k_t/k_c \Delta\pi \tag{1}$$

$$\Delta k_2 = \Delta\sigma + \Delta\pi \tag{2}$$

The results of these calculations are given in Table 3. The values of $\Delta\sigma$ range between -0.62 and -1.03 while those of $\Delta\pi$ vary between 0.48 and 0.52. There is no significant change in the $\Delta\pi$ parameters as a function of the porphyrin macro-

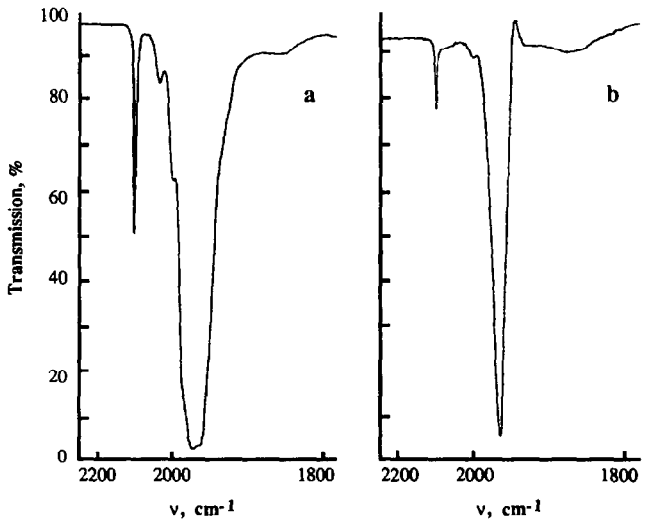

Fig. 1. Infrared spectra for (TPP)GaRe(CO)$_5$: a, as a 1% dispersion in CsI; and b, in benzene. Only the carbonyl stretching region of the spectrum is shown.

Table 2

Solid state IR data for (P)MRe(CO)$_5$ complexes (1% dispersion in CsI pellets) [a]

Porphyrin, P	Central metal, M	ν_{CO}, cm^{-1}						δ_{ReCO}, cm^{-1}		ν_{ReC}, cm^{-1}
OEP	Al	2087m	2036w	1982s	1974s	1950s	1942w	594m	588m	405w
	Ga	2088m	2039w	1982s	1976s	1960s	1944w	596m	591m	409w
	In	2090m	2042w	1986s	1979s	1966s	1946w	596m	591m	408w
	Tl	2104m	2033w	2007s	2002s	1977s	1967w		588m	394w
TPP	Ga	2096m	2041w	1995vs	1982vs	1974s		598m	589m	408w
	In	2097m	2041w	1999vs	1984vs	1976vs		599m	588m	409w
	Tl	2114m	2040w	2012vs	1999vs			593m	585m	392w

[a] Relative intensities: weak: w; medium: m; strong: s; very strong: vs.

Table 3

Solution IR data for (P)MRe(CO)$_5$ complexes in benzene with calculated force constants, Graham parameters and residual charges

Porphyrin, P	Central metal, M	ν_{CO}, cm^{-1}			Force constants, [b] mdyn/Å			Graham parameters, [d] mdyn/Å		Residual charge, electron
		ν_1	ν_2	ν_m [a]	k_1	k_2	k [c]	$\Delta\sigma$	$\Delta\pi$	
OEP	Al	2088m	1987s	2012	16.11	16.44	0.25	−0.98	0.52	0.12
	Ga	2087m	1981s	2008	16.02	16.37	0.26	−1.03	0.50	0.15
	In	2093m	1982s	2010	16.05	16.41	0.27	−0.98	0.49	0.13
	Tl	2109m	2006s	2032	16.42	16.76	0.26	−0.65	0.51	~0
TPP	Ga	2095m	1982s	2010	16.05	16.42	0.28	−0.96	0.48	0.13
	In	2095m	1985s	2013	16.09	16.46	0.27	−0.92	0.48	0.11
	Tl	2113m	2005s	2037	16.41	16.77	0.27	−0.62	0.49	~0

[a] $\nu_m = 1/4(\nu_1 + 3\nu_2)$. [b] Calculated by Cotton–Kraihanzel method (see ref. 26). [c] k = interaction constant, $k = k_i = k_c = k'_c = k_t/2$ (see ref. 25). [d] Reference compound is $(CH_3)Re(CO)_5$ (see ref. 16).

cycle or of the group 13 central metal. The $\Delta\sigma$ values are also independent of both the porphyrin macrocycle and the central metal ion for complexes with M = Al, Ga, or In but not for those with M = Tl. The values of $\Delta\sigma$ parallel the electronegativities of the group 13 central metals and in this regard Tl differs substantially from Al, Ga, or In. The $\Delta\sigma$ parameters in Table 3 are similar to $\Delta\sigma$ values for complexes in the (P)MMn(CO)$_5$ series, but the $\Delta\pi$ parameters of (P)MRe(CO)$_5$ are significantly higher [30 *]. This demonstrates that the π acceptor character of the main group metalloporphyrin unit increases when it is σ-bonded to a Re(CO)$_5$ group.

Calculated residual charges agree with trends deduced from Graham's parameters [31]. The thallium–rhenium bond of (P)TlRe(CO)$_5$ is predominantly covalent as is the thallium–manganese bond of (P)TlMn(CO)$_5$. The bond polarization is less for (P)TlRe(CO)$_5$ than for (P)MRe(CO)$_5$ where M = Al, Ga, or In, which all have a residual charge of about 0.1 electron. In addition, the UV-visible spectroscopic data indicate that the metal–metal covalent bond character in (P)MRe(CO)$_5$ is larger than in (P)MCo(CO)$_4$ or (P)MM′(CO)$_3$Cp where M′ = Cr, Mo or W.

The UV-visible spectra of (OEP)GaRe(CO)$_5$ and (OEP)TlRe(CO)$_5$ in benzene are illustrated in Figure 2. Similar spectra are obtained for each (P)MRe(CO)$_5$ complex and data for these species are summarized in Table 4. Two bands appear in

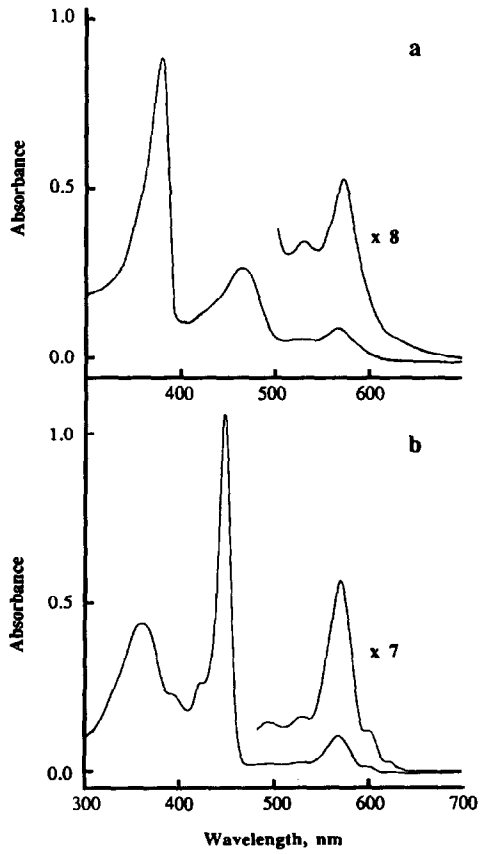

Fig. 2. UV-visible spectra of: a, (OEP)GaRe(CO)$_5$; and b, (OEP)TlRe(CO)$_5$ in benzene.

Table 4

UV-visible data for (P)MRe(CO)$_5$ complexes in benzene (λ, nm; ϵ, M^{-1} cm^{-1})

Porphyrin, P	Central metal, M	λ_{max} (10^{-3} ϵ)					ϵ(II)/ϵ(I)	
		Soret region		Q bands			(P)MRe(CO)$_5$	(P)M(CH$_3$) [a]
		Band I	Band II	Q(2,0)	Q(1,0)	Q(0,0)		
OEP	Al	386 (87.0)		534 (6.2)	572 (7.7)	600 (1.3)	~ 0	4.22
	Ga	382 (92.6)	472 (23.4)	534 (1.3)	572 (7.2)		0.25	4.45
	In	377 (91.3)	453 (66.0)	530 (1.5)	564 (14.0)	594 (3.1)	0.72	5.04
	Tl	364 (42.8)	451 (131.2)	530 (1.2)	568 (13.0)	600 (2.3)	3.07	6.00
TPP	Ga	393 (123.2)	472 (59.4)	550 (1.4)	595 (3.7)	649 (7.7)	0.48	12.91
	In	387 (61.2)	459 (135.0)	549 (2.5)	590 (6.7)	637 (10.9)	2.21	13.74
	Tl	355 (23.3)	457 (241.3)	550 (1.8)	594 (7.3)	640 (12.9)	10.37	15.20

[a] From refs. 10, 11, 33, and 34.

the Soret region of the spectrum. Band I appears between 355 and 393 nm while Band II (the Soret band) is located between 451 to 472 nm. Band I shifts towards the blue with changes in the porphyrin central metal and this shift follows the sequence: Tl < In < Ga < Al. A blue shift in the Soret band absorption is also observed for the Ga, In and Tl complexes but this band is too weak to be observed for (OEP)AlRe(CO)$_5$. The Band I absorption is attributed to an $np_z \rightarrow e_g(\pi^*)$ transition while Band II is assigned as a $\pi \rightarrow \pi^*$ transition of the porphyrin macrocycle [32].

Changes in the molar absorptivity ratio of a given (P)MM'(L) complex, ϵ(II)/ϵ(I), can occur upon modification of the porphyrin π system electron density and will vary substantially with the electron-withdrawing character of the central metal [7,8]. The electronic absorption spectra of (P)MRe(CO)$_5$ belong to the hyperclass and the ϵ(II)/ϵ(I) ratios follow the trend: Tl > In > Ga > Al. The same order is observed for group 13 porphyrins of the type (P)M(CH$_3$) [10,11,33,34] and molar absorptivity ratios, ϵ(II)/ϵ(I), for these σ-bonded complexes are also listed in Table 4.

Figure 3 shows a linear correlation between the metal ion electronegativity and ϵ(II)/ϵ(I) for compounds in the (P)MRe(CO)$_5$ and (P)M(CH$_3$) series. As expected, the charge transfer from the central metal to the porphyrin macrocycle decreases when the metal electronegativity of (P)MRe(CO)$_5$ or (P)M(CH$_3$) increases. The ϵ(II)/ϵ(I) ratios of complexes in the OEP series are smaller than those for TPP derivatives containing the same σ-bonded axial ligand, and this is consistent with the more basic OEP macrocycle. In addition, the slope of ϵ(II)/ϵ(I) vs electronegativity is much higher for (TPP)MRe(CO)$_5$ than for the other three series of complexes plotted in Figure 3. This correlation parallels the relative stability of each investigated (P)MRe(CO)$_5$ complex.

A correlation of ϵ(II)/ϵ(I) with metal electronegativity has previously been reported by our group for (P)M(R) [10,11,33,34] and the same type of correlations for metal–metal bonded complexes indicates that the metalate anions exhibit greater electron-donating properties than either the alkyl or the aryl groups. The only exceptions noted to date are the C(CH$_3$)$_3$ ligands, and the ϵ(II)/ϵ(I) ratio for a given metal–metal or metal–carbon bonded species decreases according to the following sequence of axial ligands:

$$C(CH_3)_3 > Re(CO)_5 \approx Mn(CO)_5 > Cr(CO)_3Cp > Mo(CO)_3Cp > W(CO)_3Cp > Co(CO)_4 > CH_3 > C_6H_5 > C_6F_4H \approx C_6F_5$$

Figure 4 illustrates the ^{1}H NMR spectra of (OEP)AlRe(CO)$_5$ in C_6D_6. The data for this compound, as well as that for the other (P)MRe(CO)$_5$ derivatives are listed in Table 5. All of the spectra are typical of diamagnetic metalloporphyrins. The *meso* proton chemical shifts of the OEP complexes range between 10.35 and 10.44 ppm and are diagnostic of complexes containing trivalent central metals [35]. The methylenic and methylic protons of the octaethylporphyrin complexes have multiplet and triplet signals in the range of 3.98 to 4.07 ppm and 1.88 to 1.91 ppm, respectively (see Figure 4 and Table 5). The methylenic protons of the Al, Ga, and In derivatives are anisochronous and their signal results from an ABX$_3$ coupling. A methylenic proton inequivalence is not observed for the thallium derivatives but occurs for the other three (OEP)MRe(CO)$_5$ derivatives and increases in the order In < Ga < Al. A solvent effect cannot be invoked. However, previous work on indium [6,7,9,36] and thallium [8] σ-bonded porphyrins has shown that carbonyl

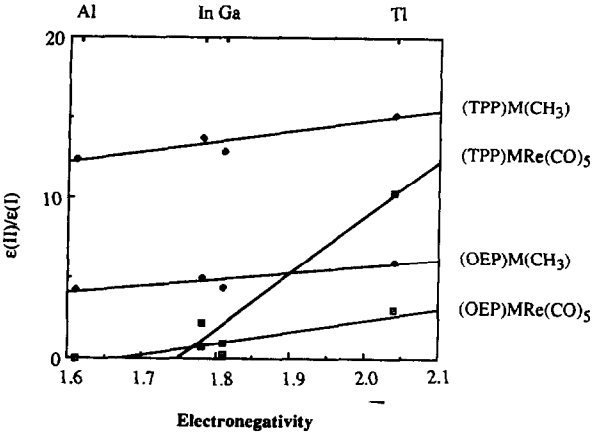

Fig. 3. Correlation of $\epsilon(II)/\epsilon(I)$ ratio vs. the porphyrin central metal electronegativity for $(P)MRe(CO)_5$ and $(P)M(CH_3)$.

metalate ligands such as $Mn(CO)_5$ and $Co(CO)_4$ induce a much smaller inequivalence of the porphyrin plane than does $M(CO)_3Cp$. Thus, the local symmetry of the axial ligand can be responsible for the methylenic proton inequivalence in $(P)MRe(CO)_5$. On the other hand, the methylenic proton inequivalence of compounds in the $(OEP)M(CH_3)$ series [10,11,33,34] is almost constant, independent of the central metal ion ($|\delta(H_A) - \delta(H_B)| \approx 4$ Hz). Consequently, the methylenic proton anisochrony for complexes in the $(OEP)MRe(CO)_5$ series must be explained by the distance from the equatorial carbonyl plane to the proton sites. This is also suggested by structural data of $(OEP)InMn(CO)_5$ [7], $(OEP)TlMn(CO)_5$ [8] and $(OEP)SnFe(CO)_4$ [37].

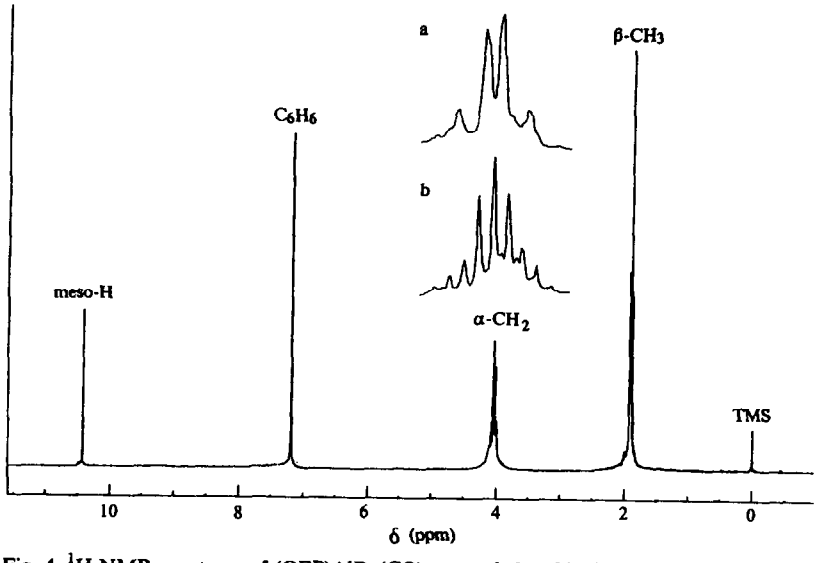

Fig. 4. ^1H NMR spectrum of $(OEP)AlRe(CO)_5$ recorded at 294 K in C_6D_6. The insert shows the α-CH_2 protons; a, with decoupling of the methyl protons; and b, without decoupling.

Table 5

^{1}H NMR data [a] for (P)MRe(CO)$_5$ complexes

Porphyrin, P	Central metal, M	R^1	R^2	Protons of R^1	multi/i	δ	Protons of R^2	multi/i	δ
OEP	Al	H	C_2H_5	*meso*-H	s/4	10.40	β-CH_3	t/24	1.88
							α-CH_2	m/8	4.03
							α'-CH_2	m/8	3.98
	Ga	H	C_2H_5	*meso*-H	s/4	10.42	β-CH_3	t/24	1.89
							α-CH_2	m/8	4.07
							α'-CH_2	m/8	4.03
	In	H	C_2H_5	*meso*-H	s/4	10.44	β-CH_3	t/24	1.90
							α-CH_2	m/16	4.05
	Tl	H	C_2H_5	*meso*-H	s/4	10.35	β-CH_3	t/24	1.91
							α-CH_2	q/16	4.06
TPP	Ga	C_6H_5	H	*o*-H	br/4	8.30	pyrr-H	s/8	9.08
				o'-H	br/4	8.10			
				m,p-H	m/12	7.50			
	In	C_6H_5	H	*o*-H	br/4	8.36	pyrr-H	s/8	9.09
				o'-H	br/4	8.10			
				m,p-H	m/12	7.52			
	Tl	C_6H_5	H	*o*-H	br/4	8.34	pyrr-H	s/8	9.09
				o'-H	br/4	8.14			
				m,p-H	m/12	7.52			

[a] Spectra were recorded in C_6D_6 at 21°C with $SiMe_4$ as internal reference; chemical shifts downfield from $SiMe_4$ are defined as positive. Abbreviations: R^1 = porphyrin methinic group; R^2 = porphyrin pyrrole group; multi = multiplicity; i = intensity; s = singlet; d = doublet; t = triplet; q = quartet; m = multiplet; br = broad peak.

Finally, it should be noted that, in contrast to (OEP)MRe(CO)$_5$, the differences between the *o*-H and *o'*-H chemical shifts in (TPP)MM'(L) are constant and close to 0.2 ppm. This agrees with pentacoordination of the porphyrin metal as well as with a slow phenyl group rotation. It is also consistent with a weak porphyrin plane asymmetry which is induced by the M'(CO)$_n$ carbonyl ligand of (TPP)MM'(CO)$_n$.

Electrochemistry of (P)MRe(CO)$_5$. The electrochemistry of each (P)MRe(CO)$_5$ derivative was investigated in CH_2Cl_2 containing 0.1 *M* TBA(PF_6). Two electroreductions are observed for each TPP complex. In contrast, the four OEP derivatives are reduced via a single one-electron transfer step over the cathodic potential range of the solvent. All of the reductions except for those of (TPP)TlRe(CO)$_5$ and (OEP)TlRe(CO)$_5$ are reversible.

Cyclic voltammograms for (TPP)MRe(CO)$_5$ where M = Ga, In or Tl (the Al derivative could not be isolated) are illustrated in Figure 5 while half wave or peak potentials for oxidation and reduction of the seven investigated metal–metal bonded derivatives are summarized in Table 6. The absolute potential difference between the first and second reduction of (TPP)GaRe(CO)$_5$ is 0.37 V in CH_2Cl_2 while the $\Delta E_{1/2}$ between the same two reactions of (TPP)InRe(CO)$_5$ is 0.43 V. Both values are in agreement with observed separations when the electrode reactions involve

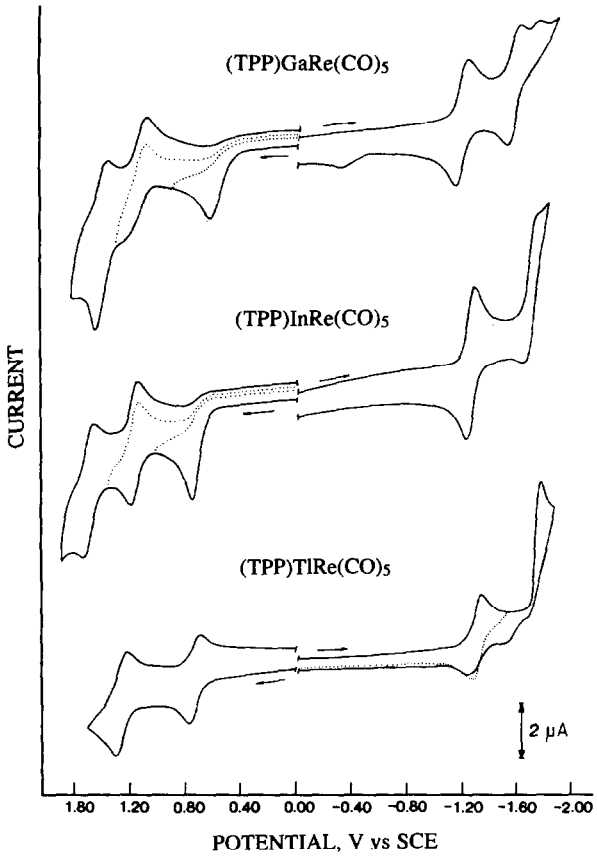

Fig. 5. Cyclic voltammograms of (TPP)GaRe(CO)$_5$ (TPP)InRe(CO)$_5$, and (TPP)TlRe(CO)$_5$ in CH_2Cl_2, 0.1 *M* TBA(PF_6).

Table 6

Half-wave and peak potentials (V vs SCE) for the oxidation and reduction of (P)MRe(CO)$_5$ and (P)M(CH_3) in CH_2Cl_2, 0.1 *M* TBA(PF_6). Unless otherwise noted all listed potentials correspond to reversible $E_{1/2}$ values

Compound	Metal, M	Reduction		Oxidation		
		1st	2nd	1st	2nd	3rd
(TPP)MRe(CO)$_5$	Ga	−1.19	−1.56	0.64 [a]	1.17	1.45
	In	−1.26	−1.69	0.76 [a]	1.17	1.50
	Tl	−1.32	−1.77 [a]	0.73	1.26	–
(OEP)MRe(CO)$_5$ [c]	Al	−1.48	–	0.50 [a,b]	0.65 [b]	0.89 [b]
	In	−1.52	–	0.73 [a]	1.10	1.43
	Tl	−1.66 [a]	–	0.67	1.07	–

[a] Peak potential obtained at 0.1 V/s. [b] Peak not well defined. [c] (OEP)GaRe(CO)$_5$ decomposes in the presence of supporting electrolyte to give (OEP)Ga(PF_6) and values of $E_{1/2}$ are therefore not given in the Table.

formation of a porphyrin π anion radical and dianion ($\Delta E_{1/2} = 0.42 \pm 0.05$ V) [38] as shown by equations 3 and 4 where M = Ga or In.

$$(TPP)MRe(CO)_5 + e \rightleftharpoons [(TPP)MRe(CO)_5]^{-\cdot} \quad (3)$$

$$[(TPP)MRe(CO)_5]^{-\cdot} + e \rightleftharpoons [(TPP)MRe(CO)_5]^{2-} \quad (4)$$

The electroreduction of $(TPP)TlRe(CO)_5$ differs slightly from that of $(TPP)GaRe(CO)_5$ and $(TPP)InRe(CO)_5$. The latter two species are reduced in two reversible one-electron transfer steps while $(TPP)TlRe(CO)_5$ undergoes an initial reversible reduction ($E_{1/2} = -1.32$ V) which is followed by a second irreversible reduction located at $E_p = -1.77$ V. The peak to peak potential difference, $|E_{pa} - E_{pc}| = 60 \pm 5$ mV, as well as the constant value of $i_p/v^{1/2}$ for the first reduction of $(TPP)TlRe(CO)_5$ indicate a diffusion controlled one electron transfer process. The difference in half wave potentials between the first oxidation and the first reduction of this complex is 2.05 ± 0.05 V, and this agrees with the 2.25 ± 0.15 V separation generally observed for porphyrin ring centered oxidations and reductions [2,38].

The electrooxidation of $(TPP)TlRe(CO)_5$ in CH_2Cl_2 also differs from $(TPP)InRe(CO)_5$ and $(TPP)GaRe(CO)_5$ in that the σ-bonded Tl complex undergoes two reversible reactions (located at $E_{1/2} = 0.73$ and 1.26 V). No cleavage of the Tl–Re bond occurs after the abstraction of one or two electrons and the electro-oxidized species are stable on the cyclic voltammetric time scale. A stability of singly and doubly oxidized σ-bonded thallium–carbon porphyrins has also been observed [34].

$(TPP)GaRe(CO)_5$ and $(TPP)InRe(CO)_5$ both undergo three oxidations in CH_2Cl_2 containing 0.1 *M* $TBA(PF_6)$. The initial oxidation is not coupled to a return reduction peak (see Figure 5) but the shape of the current voltage curve, $|E_p - E_{p/2} = 65 \pm 5$ mV, is consistent with a diffusion controlled one electron transfer. The second and the third oxidations of both compounds occur at similar potentials which are almost identical to those for the oxidation of (TPP)GaCl [11] or (TPP)InCl [39] in CH_2Cl_2. These data are consistent with the initial reversible oxidation of $(TPP)MRe(CO)_5$ being followed by a rapid cleavage of the metal–metal bond. The following two oxidations involve reactions of homogeneously generated $[(P)M^{III}]^+$ and the overall conversion of $(TPP)MRe(CO)_5$ to $[(P)M^{III}]^{3+}$ occurs as shown in equations 5 to 8.

$$(P)M^{III}Re(CO)_5 \rightleftharpoons [(P)M^{III}Re(CO)_5]^{+\cdot} + e \quad (5)$$

$$[(P)M^{III}Re(CO)_5]^{+\cdot} \rightarrow [(P)M^{III}]^+ + Re(CO)_5^{\cdot} \quad (6)$$

$$[(P)M^{III}]^+ \rightleftharpoons [(P)M^{III}]^{2+} + e \quad (7)$$

$$[(P)M^{III}]^{2+} \rightleftharpoons [(P)M^{III}]^{3+} + e \quad (8)$$

Similar types of current–voltage curves are obtained for oxidation of $(OEP)AlRe(CO)_5$ and $(OEP)InRe(CO)_5$, both of which undergo an oxidation mechanism of the type shown in equations 5–8. However, cyclic voltammograms for these two compounds differ from those of $(OEP)GaRe(CO)_5$ which has redox potentials similar to (OEP)GaCl in CH_2Cl_2 [11]. This result indicates that $(OEP)GaRe(CO)_5$ undergoes a cleavage of the metal–metal bond to give $(OEP)Ga(PF_6)$ in the presence of supporting electrolyte.

The electrochemistry of (OEP)TlRe(CO)$_5$ is similar to that of (TPP)TlRe(CO)$_5$ in that both oxidations of the OEP complex are reversible. However, the two compounds differ somewhat in that the OEP derivative is irreversibly reduced (see top cyclic voltammogram in Figure 6b) while the TPP derivative is reversibly reduced on the cyclic voltammetry timescale (see Figure 5). The single reduction peak of both complexes has an $|E_p - E_{p/2}| = 65 \pm 5$ mV, and this is consistent with a diffusion controlled one electron transfer step. The σ-bonded (OEP)Tl(R) species all undergo reduction at the metal center [34] and this may also be the case for the initial reduction of (OEP)TlRe(CO)$_5$.

Finally, it should be noted that the overall electrochemistry of (P)MRe(CO)$_5$ is quite similar to that of previously characterized group 13 metal–metal and metal–carbon σ bonded porphyrins of the type (P)MM′(L) or (P)M(R) [1–3,8,10,11]. The first oxidation of derivatives with Al, Ga, or In central metals leads to unstable singly oxidized products and the electrogenerated radicals undergo a rapid cleavage of the metal–metal or metal–carbon bond to give an overall irreversible oxidation. In contrast, σ-bonded complexes of Tl can be converted to stable electrooxidation products after the abstraction of either one or two electrons from the metalloporphyrin π ring system.

Potentials for electrooxidation of Al, Ga, In, and Tl porphyrins vary with the nature of the σ-bonded axial ligand and this is best demonstrated by comparing potentials for the first oxidation of the Tl derivatives. These electrode reactions are all reversible and $E_{1/2}$ values can thus be correlated with changes in electron density at the reaction site. An example of this correlation is given in Figure 6a which plots $E_{1/2}$ for the first oxidation of each compound in a given OEP series as a function of its ϵ(II)/ϵ(I) ratio taken from the spectroscopic data [8,34]. As seen in the Figure, a linear correlation is observed as $E_{1/2}$ varies from +0.65 V for the oxidation of (OEP)TlW(CO)$_3$Cp or (OEP)TlMo(CO)$_3$Cp to $E_{1/2} = 0.88$ V for the oxidation of (OEP)Tl(C_6F_5). (OEP)TlMn(CO)$_5$ and (OEP)TlRe(CO)$_5$ both show deviation from the plot, with the largest variation being for the Mn(CO)$_5$ derivative. However, there is no difference in the shape of reversibility or oxidation peaks for the seven investigated metalloporphyrins and this is illustrated in Figure 6b by cyclic voltammograms for three representative complexes.

No apparent correlation exists between $E_{1/2}$ for reduction of the various (P)MM′(L) or (P)M(R) derivatives and the nature of the axial ligand. This is illustrated in Figure 7. The first reduction of (P)InM′(L) or (P)In(R) varies by less then 60 mV for a given complex in the OEP series and by less than 90 mV for compounds in the TPP series. Fewer data were obtained for the Ga, Tl, and Al derivatives but again no correlation is observed between $E_{1/2}$ for the first or second reduction of the metalloporphyrin and the nature of the axial ligand. For example, the difference in $E_{1/2}$ between the first reduction of (TPP)MRe(CO)$_5$ and the first reduction of (TPP)M(C_6H_5) where M = In, Ga, Al or Tl is less than 80 mV under the same experimental conditions [10,11,33,34]. Thus, the electrochemical data are all self consistent and indicate that the reduction of (P)MRe(CO)$_5$ where M = Al, Ga, or In occurs at a porphyrin π ring system whose orbitals do not significantly overlap with those of the σ-bonded Re(CO)$_5$ axial ligand. On the other hand, a large substituent effect is observed in the oxidations, and this is consistent with the electron being abstracted from orbitals which may involve the metal–metal σ-bond of (P)MRe(CO)$_5$.

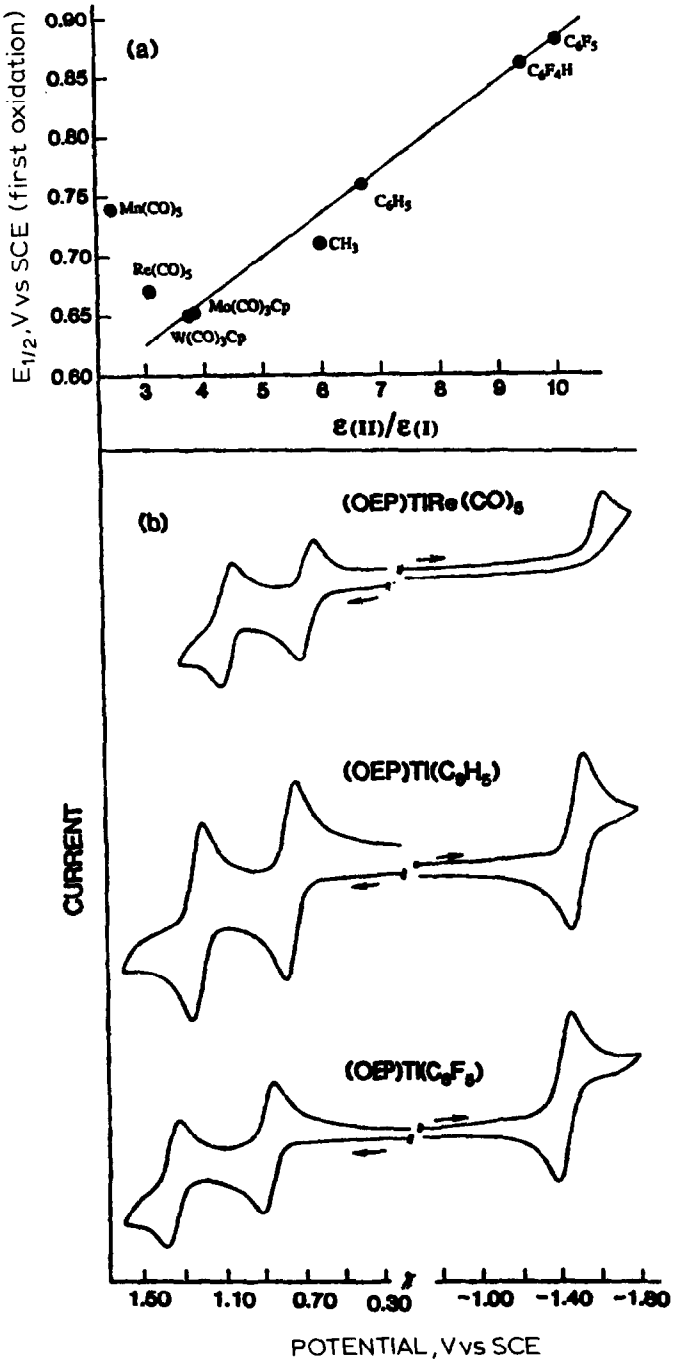

Fig. 6. (a) Correlation between half-wave potentials for the first oxidation of (OEP)TlM′(L) or (OEP)Tl(R) and the ε(II)/ε(I) ratio of the neutral complex. The specific σ-bonded ligands are shown in the plot; (b) cyclic voltammograms for the oxidation and reduction of representative σ-bonded Tl complexes in CH_2Cl_2, 0.1 *M* TBA(PF_6).

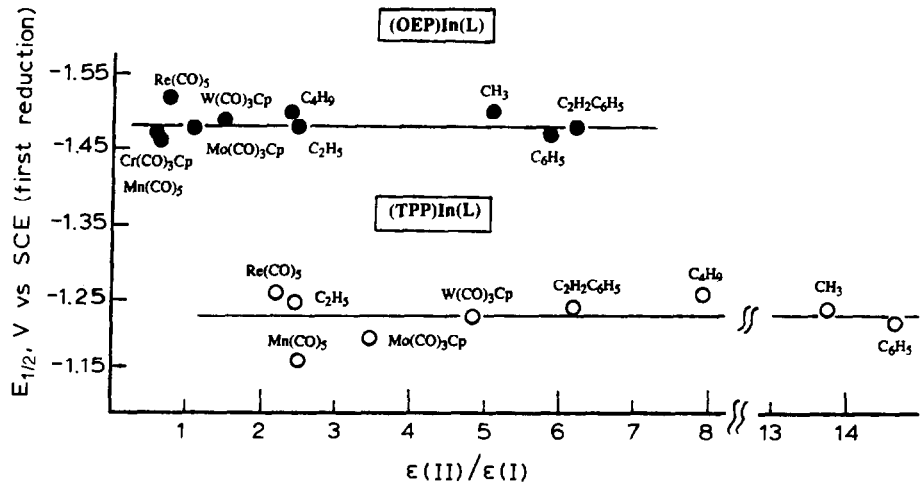

Fig. 7. Correlation of $E_{1/2}$ vs. the ϵ(II)/ϵ(I) ratio for (P)InM'(L) and (P)In(R) where P = OEP (●) or TPP (○).

Acknowledgment

The support of the C.N.R.S. and the National Science Foundation (Grant no. CHE-8822881) is gratefully acknowledged.

References

1 R. Guilard, C. Lecomte, K.M. Kadish, Struct. Bonding, 64 (1987) 205.
2 K.M. Kadish, Prog. Inorg. Chem., 34 (1986) 435–605.
3 R. Guilard, K.M. Kadish, Comments Inorg. Chem., 7 (1988) 287–305.
4 H.W. Bosch, B.B. Wayland, J. Organomet. Chem., 317 (1986) C5.
5 T. Boschi, S. Licoccia, R. Paolesse, P. Tagliatesta, Inorg. Chim. Acta, 145 (1988) 19.
6 P. Cocolios, C. Moïse, R. Guilard, J. Organomet. Chem., 228 (1982) C43.
7 R. Guilard, P. Mitaine, C. Moïse, C. Lecomte, A. Boukhris, C. Swistak, A. Tabard, D. Lacombe, J.-L. Cornillon, K.M. Kadish, Inorg. Chem., 26 (1987) 2467.
8 R. Guilard, A. Zrineh, M. Ferhat, A. Tabard, P. Mitaine, C. Swistak, P. Richard, C. Lecomte, K.M. Kadish, Inorg. Chem., 27 (1988) 697.
9 S. Onaka, Y. Kondo, M. Yamashita, Y. Tatematsu, Y. Kato, M. Goto, T. Ito, Inorg. Chem., 24 (1985) 1070.
10 R. Guilard, A. Zrineh, A. Tabard, A. Endo, B.C. Han, C. Lecomte, M. Souhassou, A. Habbou, M. Ferhat, K.M. Kadish, Inorg. Chem., 29 (1990) 4476.
11 K.M. Kadish, B. Boisselier-Cocolios, A. Coutsolelos, P. Mitaine, R. Guilard, Inorg. Chem., 24 (1985) 4521.
12 R.E. Dessy, R.L. Pohl, R.B. King, J. Am. Chem. Soc., 88 (1966) 5121.
13 D.D. Perrin, W.L.F. Armarego, D.R. Perrin, Purification of Laboratory Chemicals, Pergamon, New York, 1980.
14 (a) Y. Kaizu, N. Misu, K. Tsuji, Y. Kaneko, H. Kobayashi, Bull. Chem. Soc. Jpn., 58 (1985) 103. (b) A. Coutsolelos, R. Guilard, J. Organomet. Chem., 253 (1983) 273. (c) M. Bhatti, W. Bhatti, E. Mast, Inorg. Nucl. Chem. Lett., 8 (1972) 133. (d) K. Henrick, R.W. Matthews, P.A. Tasker, Inorg. Chem., 16 (1977) 3293.
15 J.E. Ellis, E.A. Flom, J. Organomet. Chem., 99 (1975) 263.
16 J.B. Wilford, F.G.A. Stone, Inorg. Chem., 4 (1965) 389.
17 P.S. Braterman, Struct. Bonding, 26 (1976) 1.
18 P.S. Braterman, Metal Carbonyl Spectra, Academic Press, New York, 1975.

19 K. Nakamoto, Infrared and Raman Spectra of Inorganic and Coordination Compounds, 3rd ed., Part III, Wiley, New York, 1978.
20 (OEP)InMn(CO)$_5$: δ_{MnCO} = 669, 653 cm^{-1}; ν_{MnC} = 490 cm^{-1}. (OEP)TlMn(CO)$_5$: δ_{MnCO} = 662, 648 cm^{-1}; ν_{MnC} = 472 cm^{-1}. (TPP)InMn(CO)$_5$: δ_{MnCO} = 670, 635 cm^{-1}; ν_{MnC} = 490 cm^{-1}. (TPP)TlMn(CO)$_5$: δ_{MnCO} = 660, 647, 636 cm^{-1}; ν_{MnC} = 467 cm^{-1}.
21 N. Flitcroft, D.K. Huggins, H.D. Kaesz, Inorg. Chem., 3 (1964) 1123.
22 W. Jetz, P.B. Simons, J.A.J. Thompson, W.A.G. Graham, Inorg. Chem., 5 (1966) 2217.
23 J.C. Hileman, D.K. Huggins, H.D. Kaesz, Inorg. Chem., 1 (1962) 933.
24 H.D. Kaesz, R. Bau, D. Hendrickson, J.M. Smith, J. Am. Chem. Soc., 89 (1967) 2844.
25 k_1 and k_2 are the axial and equatorial CO stretching force constants, respectively; k_c, k'_c and k_t are the interaction constants between axial–equatorial and equatorial–equatorial CO groups, respectively.
26 F.A. Cotton, C.S. Kraihanzel, J. Am. Chem. Soc., 84 (1962) 4432.
27 L.E. Orgel, Inorg. Chem., 1 (1962) 25.
28 W.A.G. Graham, Inorg. Chem., 7 (1968) 315.
29 W. Hieber, G. Braunz, Naturforsch., 14B (1959) 132.
30 (OEP)InMn(CO)$_5$: $\Delta\sigma = -0.98$, $\Delta\pi = 0.37$, residual charge ≈ 0.12 e$^-$; (OEP)TlMn(CO)$_5$: $\Delta\sigma = -0.69$, $\Delta\pi = 0.41$, residual charge ≈ 0 e$^-$; (TPP)InMn(CO)$_5$: $\Delta\sigma = -0.94$, $\Delta\pi = 0.37$, residual charge = 0.11 e$^-$; (TPP)TlMn(CO)$_5$: $\Delta\sigma = -0.63$, $\Delta\pi = 0.40$, residual charge ≈ 0 e$^-$.
31 O. Kahn, M.J. Bigorgne, J. Organomet. Chem., 10 (1967) 137.
32 M. Gouterman, in D. Dolphin, (Ed.), The Porphyrins, Vol. III, Academic, New York, 1978, Chapter I.
33 K.M. Kadish, B. Boisselier-Cocolios, P. Cocolios, R. Guilard, Inorg. Chem., 24 (1985) 2139.
34 K.M. Kadish, A. Tabard, A. Zrineh, M. Ferhat, R. Guilard, Inorg. Chem., 26 (1987) 2459.
35 H. Sheer, J.J. Katz, Porphyrins and Metalloporphyrins, K.M. Smith, Ed., Elsevier, Amsterdam, Chapter 10 (1975).
36 R. Guilard, P. Mitaine, C. Moïse, P. Cocolios, K.M. Kadish, New J. Chem., 12 (1988) 699.
37 J.-M. Barbe, R. Guilard, C. Lecomte, R. Gerardin, Polyhedron, 3 (1984) 889.
38 J.-H. Fuhrhop, K.M. Kadish, D.G. Davis, J. Am. Chem. Soc., 95 (1973) 5140.
39 K.M. Kadish, J.L. Cornillon, P. Cocolios, A. Tabard, R. Guilard, Inorg. Chem., 24 (1985) 3645.